Asian Journal of Chemistry; Vol. 35, No. 5 (2023), 1199-1204

ASIAN JOURNAL OF CHEMISTRY

https://doi.org/10.14233/ajchem.2023.27285

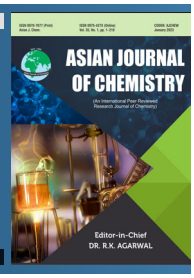

Aquatic Weed Derived SnO_2 Nanoparticle: Synthesis, Characterization and its Application for Degradation of Dyes and Wastewater Treatment

SHIVAM PANDEY[1], AJAY SINGH[1,*], WASEEM AHMAD[2], RITURAJ PANWAR[1] and SHAINA ANAND[1]

[1]Department of Chemistry, School of Applied and Life Sciences, Uttaranchal University, Dehradun-248007, India
[2]Graphic Era University, Dehradun-248007, India

*Corresponding author: E-mail: ajay21singh@yahoo.com

Received: 18 December 2022; *Accepted*: 13 April 2023; *Published online*: 28 April 2023; AJC-21229

The spread and destruction of freshwater ecosystems by aquatic invasive organisms poses a threat to economic, social and environmental processes. *Eichhornia crassipes* (Mart.) Solms, commonly known as water hyacinth, is globally distributed, toxic and floating watery plant. Its rapid development causes an abundance of the plant to float on the surface of water, reducing the amount of oxygen in water and destroying the aquatic ecosystem. Thus, its invasive growth has become a global concern. Green synthesis method was used to synthesize stannous oxide nanoparticles from water hyacinth as a precursor. The plant extract acted as a reducing agent due to presence of carboxyl, hydroxyl and carbonyl groups. The UV-Vis analysis, XRD, SEM coupled with EDX and FT-IR were utilized for characterization of the nanoparticles. The results indicated that the nanoparticles produced have high potential to degrade the methyl orange and methylene blue dyes. The use of metal nanoparticles has also shown reduction of various pollutants varying from 60-90% in wastewater. When the concentration of these nanoparticles was doubled, they were found to be more effective under optimized conditions from wastewater.

Keywords: Nanoparticles, Stannous nanoparticles, Water hyacinth, Aquatic weed, Wastewater treatment, Water pollutants.

INTRODUCTION

The Sustainable Development Goals (SDGs) are the latest initiative from the international community that involves states and non-governmental organizations to boost the living standards of billions of people. The objectives are ambitious, demanding necessary action plan for the "people, planet and prosperity" by year 2030 [1]. Within agenda of its Development Goals, the United Nations has made 2030 as target year to provide the universal and equitable access to provide safe and cheap potable water for all people, but the progress toward this goal of 2030 is still being made very slowly. Because of this, water treatment has become one of the most important components in the process of achieving sustainable water supplies [2-4]. The treatment of wastewater contributes to almost 11 of the 17 sustainable development goals. The most significant contribution is its capacity to boost water availability, improve global human health, provide new source of revenue, convert waste to electricity and reduce wastewater's environmental effect [5].

Wastewater is generally produced every day as a byproduct of wide variety of activities, including domestic, agricultural and industrial processes and carry massive and complex chemical compositions [6,7]. The effluents produced by these various industries comprises of heavy metals, nitrogenous organics, organic carbon and other inorganics in addition to suspended and dissolved particles [8,9]. Common wastewater treatment sub-processes include coagulation, flocculation, adsorption, ionic exchange, precipitation, photodegradation, biological, membrane separation, *etc.* [10]. These wastewater treatment technologies have significant energy requirements, excess sludge discharge, carbon emissions and possess high maintenance costs. Thus, clean water and aquatic ecosystems need eco-friendly and affordable treatment [11].

The use of nanotechnolgy is now being investigated in various processes and as a potentially useful technology. It has already exhibited impressive achievements in a variety of sectors, including the treatment of wastewater. Due to their diminutive size, vast surface area and simplicity of functionalization, nanostructures provide unrivalled prospects for the production of more efficient catalysts and redox active media for the purification of wastewater [12]. It has been shown that nanomaterials are very efficient in removing variety of pollutants from the

This is an open access journal, and articles are distributed under the terms of the Attribution 4.0 International (CC BY 4.0) License. This license lets others distribute, remix, tweak, and build upon your work, even commercially, as long as they credit the author for the original creation. You must give appropriate credit, provide a link to the license, and indicate if changes were made.

wastewater, including organic and inorganic solvents, colour, biological toxins, heavy metals and pathogens that are responsible for illnesses like cholera and typhoid [13-18].

A number of studies have shown that aquatic plants can also remove both inorganic and organic pollutants [19-21]. *Eichhornia crassipes* also known as water hyacinth, is a freely floating persistent herbaceous plant with phytoremediation and bioenergy potential. According to literature, water hyacinth gasification is excellent for bioenergy generation because of its high carbon content and heating value [22]. It is among the most bothersome weed in tropical and temperate regions, since it covers many lakes, rivers and ponds throughout the world, this floating weed has been identified as an aquatic nuisance [23]. Water hyacinth's negative consequences are intimately tied to its ability to proliferate and spread quickly [24].

Due to its high-water index, *E. crassipes* ferments quickly and can supply biomass for biogas production [25,26]. Because of the distinct characteristics it has in comparison to those of other aquatic species, water hyacinth can remove harmful toxins from the surrounding water as well. According to Zhang *et al.* [27], water hyacinth is composed of structural carbohydrates such as lignin, cellulose and hemicellulose polymer and plays an important role as catalyst in the process of adsorption of water pollutants on the plant derived adsorbents [28].

In view of these optimistic qualities of water hyacinth, an attempt has been made to synthesize stannous oxide nanoparticles from water hyacinth as a precursor and also characterized by different techniques and tested its efficiency towards the degradation of methyl orange and methylene blue dyes as well as the treatment of wastewater.

EXPERIMENTAL

The plant samples of water hyacinth were collected from the river of Assan Barrage near Dakpathar, India (30º26′09″N, 77º39′56″E). The samples (leaves) were washed properly, dried and then cut into small pieces. The ethanolic extract of the leaves was then obtained by using Soxhlet apparatus and later vaporized using hot plate for 10-15 min.

Synthesis of SnO_2 nanoparticles: Stannous chloride (0.1 M, Rankem) was prepared in double distilled water, then 50 mL of solution was placed on magnetic stirrer to which 10 mL of extract was added gradually. The solution was left to stir for 4-5 h at 60 ºC. The colour change of the solution showed the formation of nanoparticles [29]. The formed particles were then kept in hot air oven for 2-3 h to dry and then the fine powdered nanoparticles were obtained.

Mechanism: The mechanism of obtained SnO_2 nanoparticles can be better understood by the following equations:

$$SnCl_2{\cdot}2H_2O + H_2O \longrightarrow Sn(OH)Cl + HCl + 2H_2O \quad (1)$$

$$Sn(OH)Cl + H_2O \longrightarrow Sn(OH)_2 + HCl \quad (2)$$

$$Sn(OH)_2 + O_2 \longrightarrow 2\ SnO_2 + 2\ H_2O \quad (3)$$

The formation of stannous oxide nanoparticles starts from the initial salt taken *i.e.* $SnCl_2$ which hydrolyzes and replaces the metal salt with hydroxyl group of water ($OH^•$). The hydrochloric acid and water molecules are obtained as byproducts, after the completion of this reaction. This hydrolysis continously separates the chlorine atoms. And, in the last step, the $Sn(OH)_2$ molecule produces water while reacting with oxygen leaving stannous oxide (SnO_2) as the end product of reaction [30].

Antimicrobial activity: The synthesized SnO_2 nanoparticles were also examined for their antioxidant activity by the well-known DPPH method. The antioxidant activity of the nanoparticles was compared to that of ascorbic acid. The free radical scavenging activity (%) was determined by using eqn. 4:

$$\text{Scavenging (\%)} = \frac{P_C - P_S}{P_C} \times 100 \quad (4)$$

where P_C = absorbance of the control, P_S = absorbance of the ascorbic acid in nanoparticles.

RESULTS AND DISCUSSION

Water hyacinth (*Eichhornia crassipes*), a well-known floating, toxic aquatic plant is found all over the world. The goal of this study was to use *Eichhornia crassipes* leaf extract to prepare stannous oxide nanoparticles. The plant acted as a reducing agent and its natural fibres assisted in keeping the particles in place during the process. The UV-Vis, XRD, SEM-EDAX and FTIR were utilized to characterize the green synthesized nanoparticles.

UV-visible studies: After every intervals of 1 h, the synthesized SnO_2 nanoparticle formation was monitored using UV-visible spectroscopy. The absorbance of the reaction was measured in the range of 200 to 800 nm. The formation of SnO_2 nanoparticles was indicated by a gradual transition from a clear mixture to a precipitated one as time progressed (Fig. 1). With the absorption edge shifting to higher energy as the particle size decreases, the absorption edge sample was found to have a value of 314 nm.

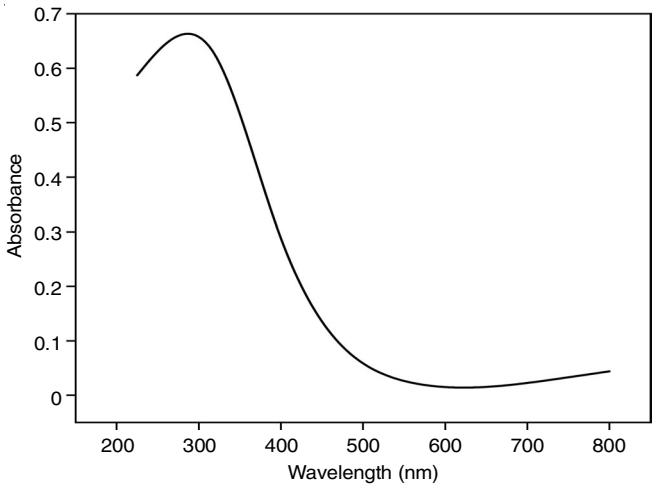

Fig. 1. UV spectrum of formed nanoparticles

XRD studies: The X-ray diffraction patterns were also obtained for the SnO_2 nanoparticles synthesized using water hyacinth plant. The diffraction peaks obtained from the XRD analysis are shown in Fig. 2. Some of the prominent peaks were observed at 22.93º, 25.61º, 27.08º, 31.09º and 40.29º.

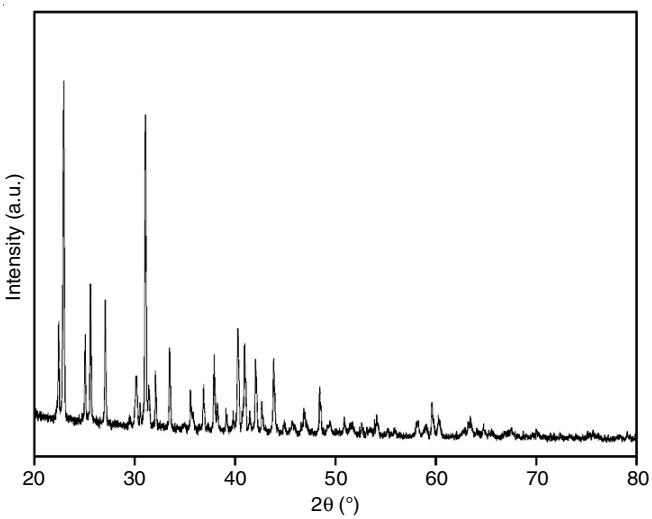

Fig. 2. X-ray diffraction image of synthesized SnO_2 nanoparticles

FTIR studies: The FTIR spectrum of SnO_2 nanoparticles have the major peaks at 3196.83, 2925.10, 1610.42, 1404.84, 1366.18 and 1097.32 cm^{-1} (Fig. 3). According to FTIR, stannous materials have strong vibrations in the range of 3500 to 2500 cm^{-1}.

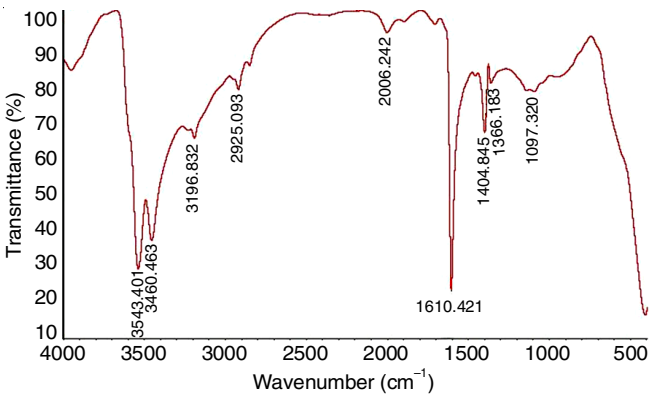

Fig. 3. FTIR of synthesized SnO_2 nanoparticles

Morphological studies: The SEM images of the synthesized nanoparticles using water hyacinth leaf extract are shown in Fig. 4. Agglomeration was observed in the obtained SnO_2 nanoparticles, which may have resulted from the powder being annealed at a low temperature. The EDX spectrum showed the presence of Sn, Cl and O, where Sn and O account for 59.48% and 35.72 wt.%, respectively while Cl was 3.20 wt.%, perhaps because of the chloride solution that was employed.

Degradation studies

Photocatalytic activity: Synthesized SnO_2 nanoparticles were used for degrading methyl orange and methylene blue dyes in the simulated solar light. About 30 min of dark agitation was allowed for the desorption-adsorption equilibrium. The experiment was then exposed to light and the changes in the absorbance maxima were monitored using a double beam spectrophotometer (Systronics India Ltd.) at set intervals. After set period of intervals, the samples were spectrophotometrically evaluated and absorbance maxima was evaluated which was

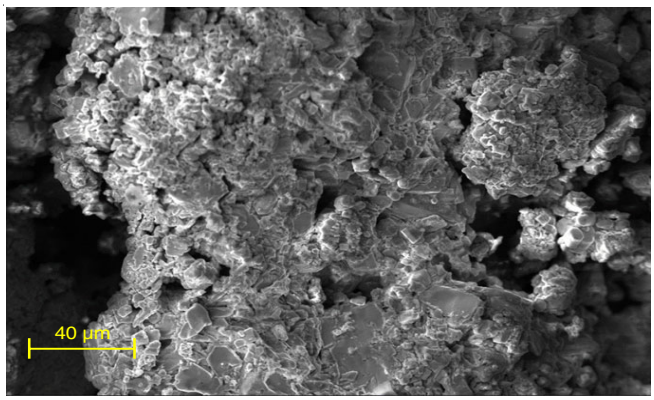

Fig. 4. SEM image of synthesized SnO_2 nanoparticles

found to be decreased with time. The degradation (%) was calculated using eqn. 5:

$$\text{Degradation (\%)} = \frac{C_f - C_i}{C_i} \times 100 \quad (5)$$

where C_i = initial concentration and C_f = final concentration.

Optimization of parameters

Dose concentration: Under simulated solar light, 10, 20, 30, 40 and 50 mg of SnO_2 nanoparticles were used to degrade both methyl orange and methylene blue dyes solutions. Fig. 5 demonstrates that initially as the catalyst dose increased, the percentage of degradation increases and at 20 mg of catalyst, the highest degradation activity was observed. The pH of both the solutions was maintained at pH-6 before starting the experiment and was not maintained later on throughout the experiment. A decrease in the percentage of degradation for both methyl orange and methylene blue dyes can be attributable to the fact that a larger catalyst dose results in blocking of light, which diminishes the photocatalytic activity. The maximum percentage of degradation was determined to be 97.23% for methyl orange solution and 95.67% for methylene blue.

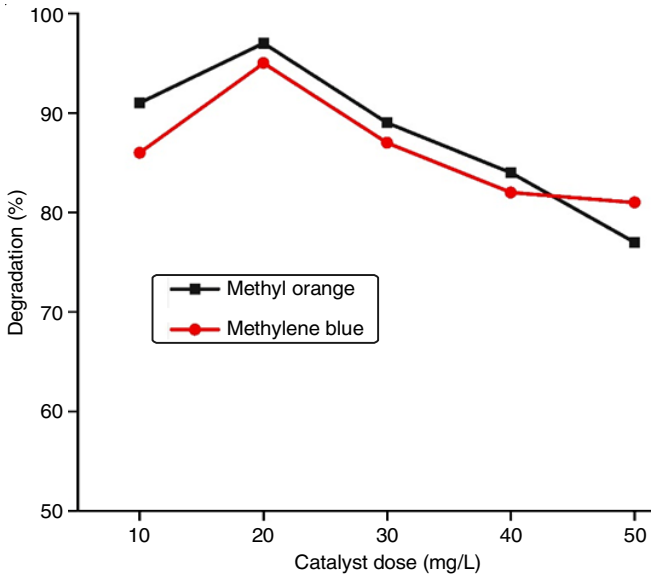

Fig. 5. Effect of varying catalytic dosage on degradation of methyl orange and methylene blue (Experimental conditions: time: 120 min, conc.: 10 ppm)

Concentration of dye: The photocatalytic activity of the SnO_2 nanoparticles was evaluated by applying 20 mg of catalyst (optimum dose) at different concentrations of 5, 10, 15, 20, 25, 30, 35 and 40 ppm of methyl orange and methylene blue dyes solutions. It was also found that the dye concentration had significant effects on the photocatalytic activity. Fig. 6 depicts a gradual decline in the photocatalytic activity following an increase in the activity up to 20 ppm, as a result of further increases in the concentration. The highest levels of photocatalytic activity were achieved at the concentration of 20 mM. Due to the maximum penetration of light, there is initially greater interaction between the light and the photocatalyst, but as the dye concentration increases, the dye molecules starts blocking the penetrating light, thus reducing the effectiveness of photocatalyst.

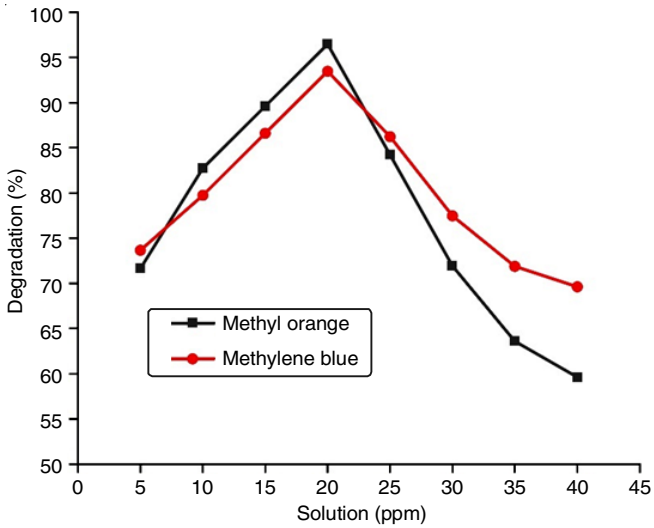

Fig. 6. Effect of varying concentration on degradation of methyl orange and methylene blue (Experimental conditions: time: 120 min, dose: 20 mg)

Effect of pH: As shown in Fig. 7, the photocatalytic activity was also evaluated by increasing the pH from 4 to 12 while holding all other reaction conditions constant. Until pH 6, the response rate increased, but further increase of pH slowed down the rate of degradation. The highest degradation occurred at pH 6, suggesting that acidic media promotes degradation more effectively than alkaline media, when 20 mg SnO_2 nanoparticles were exposed to a 20 ppm solution of methyl orange and methylene blue dyes. In the presence of sunlight, when organic molecules interact with dissolved oxygen, they dissociate into an acidic medium and cause the photo-oxidation. As the pH of nano-particle's surface alters, a dispersed state develops. Moreover, van der Waals forces prevents the agglomeration and promotes dispersion since SnO_2 nanoparticles lack charge.

Antimicrobial activity: The synthesized stannous oxide nanoparticles were applied as antibacterial agents against *E. coli* and *S. aureus* by using well-known disc diffusion method. The experimental results thus obtained showed that formed nanoparticles can act as good antibacterial agents. The antibacterial activity of the synthesized nanoparticles is due to their small size as they can easily enter into the bacterial cells

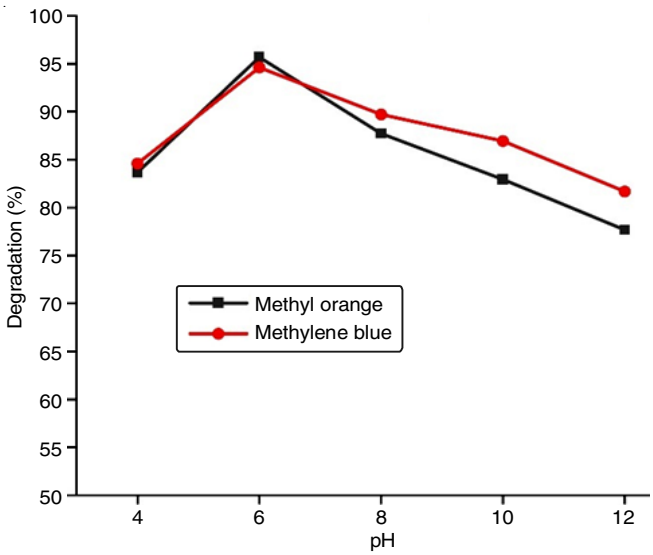

Fig. 7. Effect of varying pH on degradation of methyl orange and methylene blue (Experimental conditions: time: 120 min, conc.: 10 ppm)

and can lead to destruction of the cell membranes. After the incubation period, the zones of inhibition were found to be 24 mm and 20 mm for *E. coli* and *S. aureus*, respectively. The obtained SnO_2 nanoparticles exhibited the scavenging activity of 86.43%.

Reusability: The stability of the green synthesized SnO_2 nanoparticles as photocatalysts was also investigated in five consecutive cycles under the same reaction conditions and with the addition of fresh dye solutions to the reactor. The percentage of decomposition was recorded for all the five cycles, with a gradual decline from cycle one to cycle five. During each recycle, the catalyst was separated by centrifugation and then used for the subsequent reaction after being washed with ethanol and distilled water. The catalyst exhibited a significant activity and could be reused up to five times in a row without significant loss of the catalytic activity. This decline may be attributable to the saturation of the available surface of the catalyst, where a large number of molecules were adsorbed and prevent light from reaching the surface of SnO_2 nanoparticles, thereby reducing the electron excitation process and consequently, the generation of hydroxyl radicals and reactive oxygen species. The average result from a resusability experiment with methyl orange and methylene blue dyes is depicted in Fig. 8.

Treatment of wastewater (Applications): The prepared nanoparticles were further utilized to treat the wastewater obtained from Tons river, Dehradun, India. The pH of the wastewater changed from 4.9 ± 0.2 to 6.1 ± 0.2 during the process. Before and after the introduction of water hyacinth plant derived nanoparticles, the samples were analyzed using the standard methods as outlined by the APHA in 1995. Other parameters of the water was checked after addition of the different dosages of nanoparticles *i.e.* 0.5% and 1% and the different values are recorded in Table-1.

The results shows the better percentage removal efficiency of different water parameters like TSS, TDS, COD, BOD, nitrate and phosphate. The removal percentage was found to vary for different tested parameters. The percentage removal

TABLE-1
REDUCTION IN PARAMETERS OF WASTEWATER BY ADDITION OF 0.5% AND 1.0% TIN OXIDE NANOPARTICLES (SnO_2 NPs)

Parameters	Initial values		Values after addition of NPs		Removal efficiency (%)	
	0.5% w/w	1.0% w/w	0.5% w/w	1.0% w/w	0.5% w/w	1.0% w/w
Total suspended solids (mg/L)	115	115	44	32	61.73	72.17
Total dissolved solids (mg/L)	630	630	245	178	61.11	71.74
Chemical oxygen demand (mg/L)	557	557	202	162	63.73	70.90
Biochemical oxygen demand (mg/L)	334	334	124	99	62.87	70.35
Nitrate (mg/L)	28	28	7.4	4.3	73.58	84.64
Phosphate (mg/L)	33	33	5.9	3.2	82.13	90.30

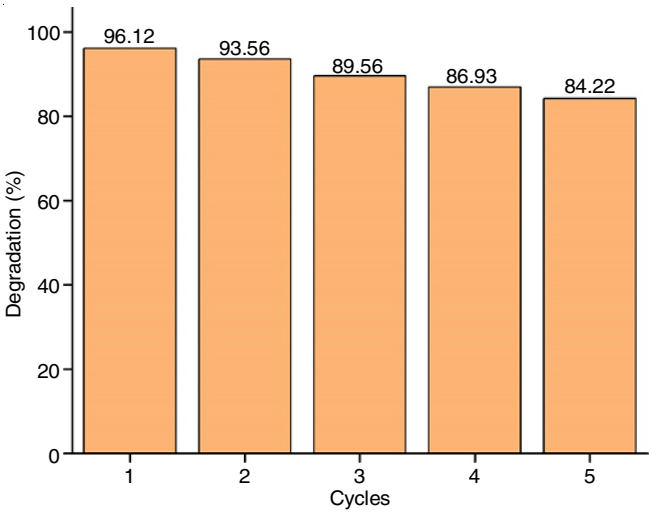

Fig. 8. Reusability of catalyst

removal of total suspended solids increased from 61.73% to 72.17%, total dissolved solids from 61.11% to 71.74%, chemical oxygen demand from 63.73% to 70.90% and biochemical oxygen demand from 62.87% to 70.35%. Moreover, the removal percentage of nitrate also increased from 73.58% to 84.64% and phosphate from 82.13% to 90.30%.

Conclusion

In this work, stannous oxide nanoparticles were prepared by using aquatic weed (*Eichhornia crassipes*) and further utilized to treat wastewater. It was found that the synthesized nanoparticles had very good removal percentage for these pollutants. The removal percentage varied from 60-90% when the dosage of the formed nanoparticles varied. Moreover, it was found that 20 mg dose of SnO_2 nanoparticles for 20 ppm of methyl orange and methylene blue dyes showed the maximum degradation of ≥ 95% for both dyes over a period of 2 h.

ACKNOWLEDGEMENTS

The authors are highly thankful to Department of Research and Innovation, Uttaranchal University, Dehradun, India for their constant support.

CONFLICT OF INTEREST

The authors declare that there is no conflict of interests regarding the publication of this article.

REFERENCES

1. United Nations, Transforming Our World: The 2030 Agenda for Sustainable Development, Department of Economic and Social Affairs, United Nations: New York (2015).
2. D. Fighir (Arsene), C. Teodosiu and S. Fiore, *Water*, **11**, 1611 (2019); https://doi.org/10.3390/w11081611
3. A. Padilla-Rivera and L.P. Güereca, *Ecol. Indic.*, **103**, 22 (2019); https://doi.org/10.1016/j.ecolind.2019.03.049
4. F. Di Maria, S. Daskal and O. Ayalon, *Ecol. Indic.*, **118**, 106805 (2020); https://doi.org/10.1016/j.ecolind.2020.106805
5. S. Pandey, B. Twala, R. Singh, A. Gehlot, A. Singh, E.C. Montero and N. Priyadarshi, *Sustainability*, **14**, 11563 (2022); https://doi.org/10.3390/su141811563
6. A.P. Tom, J.S. Jayakumar, M. Biju, J. Somarajan and M.A. Ibrahim, *Energy Nexus*, **4**, 100022 (2021); https://doi.org/10.1016/j.nexus.2021.100022
7. S. Lata and Siddharth, *Energy Nexus*, **3**, 100020 (2021); https://doi.org/10.1016/j.nexus.2021.100020
8. T. Senfter, L. Fritsch, M. Berger, T. Kofler, C. Mayerl, M. Pillei and M. Kraxner, *Carbon Resour. Convers.*, **4**, 132 (2021); https://doi.org/10.1016/j.crcon.2021.03.001
9. J. Wang, Y. Ji, F. Zhang, D. Wang, X. He and C. Wang, *Carbon Resour. Conv.*, **2**, 151 (2019); https://doi.org/10.1016/j.crcon.2019.06.001
10. A. Zaher and N. Shehata, *IOP Conf. Series Mater. Sci. Eng.*, **1046**, 012021 (2021); https://doi.org/10.1088/1757-899X/1046/1/012021
11. S. Anand, S.K. Bharti, N. Dviwedi, S.C. Barman and N. Kumar, Macrophytes for the Reclamation of Degraded Waterbodies with Potential for Bioenergy Production. In: Phytoremediation Potential of Bioenergy Plants, Springer: Singapore, pp. 333-351 (2017).
12. Z. Masood, A. Ikhlaq, A. Akram, U.Y. Qazi, O.S. Rizvi, R. Javaid, A. Alazmi, M. Madkour and F. Qi, *Catalysts*, **12**, 741 (2022); https://doi.org/10.3390/catal12070741
13. K. Jain, A.S. Patel, V.P. Pardhi and S.J.S. Flora, *Molecules*, **26**, 1797 (2021); https://doi.org/10.3390/molecules26061797
14. J. Theron, J.A. Walker and T.E. Cloete, *Crit. Rev. Microbiol.*, **34**, 43 (2008); https://doi.org/10.1080/10408410701710442
15. T. Humplik, J. Lee, S.C. O'Hern, B.A. Fellman, M.A. Baig, S.F. Hassan, M.A. Atieh, F. Rahman, T. Laoui, R. Karnik and E.N. Wang, *Nanotechnology*, **22**, 292001 (2011); https://doi.org/10.1088/0957-4484/22/29/292001
16. I. Khan, K. Saeed and I. Khan, *Arab. J. Chem.*, **12**, 908 (2019); https://doi.org/10.1016/j.arabjc.2017.05.011
17. K. Jain, Dendrimers: Smart Nanoengineered Polymers for Bioinspired Applications in Drug Delivery, In: Biopolymer-Based Composites: Drug Delivery and Biomedical Applications, Woodhead Publishing: Cambridge, U.K., pp. 169-220 (2017).
18. K. Jain, *Nanosci. Nanotechnol. Asia*, **9**, 21 (2018); https://doi.org/10.2174/2210681208666171204163622
19. A.A. Ansari, M. Naeem, S.S. Gill, F.M. AlZuaibr, *Egypt. J. Aquat. Res.*, **46**, 371 (2020); https://doi.org/10.1016/j.ejar.2020.03.002
20. H.H. Ali, M.I.A. Fayed and I.I. Lazim, *J. Glob. Innov. Agric. Sci.*, **10**, 61 (2022); https://doi.org/10.22194/JGIAS/10.985

21. S. Ali, Z. Abbas, M. Rizwan, I.E. Zaheer, I. Yavas, A. Ünay, M.M. Abdel-Daim, M. Bin-Jumah, M. Hasanuzzaman and D. Kalderis, *Sustainability*, **12**, 1927 (2020); https://doi.org/10.3390/su12051927
22. Z. Hu, X. Ma and L. Li, *Energy Convers. Manage.*, **94**, 337 (2015); https://doi.org/10.1016/j.enconman.2015.01.087
23. A. Das, P. Ghosh, T. Paul, U. Ghosh, B.R. Pati and K.C. Mondal, *3 Biotech,* **6**, 70 (2016); https://doi.org/10.1007/s13205-016-0385-y
24. M.S. Sanaa and A.S. Emad, *J. Med. Plants Res.*, **6**, 3950 (2012).
25. V.B. Barua and A.S. Kalamdhad, *J. Clean. Prod.*, **166**, 273 (2017); https://doi.org/10.1016/j.jclepro.2017.07.231
26. P. Kamaraj, R. Vennila, M. Arthanareeswari and S. Devikala, *World J. Pharm. Pharm. Sci.*, **3**, 382 (2014).
27. X. Zhang, P. Sun, K. Wei, X. Huang and X. Zhang, *Chem. Eng. J.*, **385**, 123921 (2020); https://doi.org/10.1016/j.cej.2019.123921
28. A.E. Brown, J.M. Adams, O.R. Grasham, M.A. Camargo-Valero and A.B. Ross, *Energies*, **13**, 5983 (2020); https://doi.org/10.3390/en13225983
29. N. Awoke, D. Pandey and A.B. Habtemariam, *Regen. Eng. Transl. Med.*, **8**, 407 (2021); https://doi.org/10.1007/s40883-021-00218-x
30. S.N. Matussin, A.L. Tan, M.H. Harunsani, A. Mohammad, M.H. Cho and M.M. Khan, *Mater. Chem. Phys.*, **252**, 123293 (2020); https://doi.org/10.1016/j.matchemphys.2020.123293